

Oxidative stability and oxygen permeability of oil-loaded capsules produced by spray-drying or electro-spraying measured by electron spin resonance

Nor E. Rahmani-Manglano^{a,*}, Mogens L. Andersen^b, Emilia M. Guadix^a, Pedro J. García-Moreno^{a,*}

^a Department of Chemical Engineering, University of Granada, Granada, Spain

^b Department of Food Science, University of Copenhagen, Copenhagen, Denmark

ARTICLE INFO

Keywords:

Encapsulation
Omega-3 polyunsaturated fatty acids
Electron spin resonance
Spray-drying
Monoaxial electro-spraying
Coaxial electro-spraying

ABSTRACT

The oxidative stability and the oxygen permeability of oil-loaded capsules were investigated by Electron Spin Resonance (ESR). The capsules were produced by spray-drying or electro-spraying in the monoaxial or coaxial configuration using glucose syrup as the encapsulating agent. ESR-spin trapping results showed that electro-sprayed capsules oxidized faster and during the early stages of incubation, irrespective of the emitter configuration (monoaxial or coaxial), when compared to those produced by spray-drying. Furthermore, ESR oximetry showed that oxygen inside the spray-dried capsules reached equilibrium with the surrounding atmosphere significantly slower than the monoaxially electro-sprayed capsules (i.e., ~2h and ~10 min, respectively). These findings have been attributed to the larger particle size of the spray-dried capsules influencing the oxygen diffusion area (i.e., lower surface-to-volume ratio) and diffusion path (i.e., thicker encapsulating wall for a fixed oil load). Together, the lower oxygen uptake reported for the spray-dried capsules correlated well with their higher oxidative stability.

1. Introduction

As a result of the health benefits related to the intake of omega-3 polyunsaturated fatty acids (omega-3 PUFAs), especially EPA and DHA, the enrichment of common food products with oils rich in these bioactives (e.g., fish oil) has gained great interest (Patel et al., 2022). However, stabilization techniques are required since these compounds are very prone to lipid oxidation, which may comprise the nutritional and organoleptic properties of the fortified food product. In this regard, the development of dry omega-3 delivery systems through encapsulation techniques has been a promising approach for the incorporation of these sensitive bioactive compounds into complex food matrices (Ghelichi et al., 2021).

By encapsulation, the oil is trapped within a (bio)polymer-based encapsulating wall which acts as a physical barrier between the bioactives and the environment, mainly aimed to prevent their degradation. However, lipid oxidation of the encapsulated oil still occurs. Prooxidant species, especially oxygen, have been demonstrated to penetrate through the glassy encapsulating matrix, thus triggering lipid

oxidation of the encapsulated oil droplets (A.B. Andersen et al., 2000; Boerekamp et al., 2019; Drusch et al., 2009; Orlien et al., 2000). Indeed, it has been reported that the oxidation rate of the non-continuous lipid phase embedded in a heterogeneous matrix (e.g., oil-loaded capsules) is affected by the physicochemical properties of the capsules (e.g., particle size), which influences the prooxidant species (e.g., oxygen) reaching the encapsulated oil droplets (Velasco et al., 2003, 2006).

Spray-drying of fish oil-in-water emulsions has been extensively used in the production of dry encapsulates using food-grade (bio)polymers (e.g., carbohydrates) as encapsulating agents (Singh et al., 2022). Moreover, the performance of spray-dried omega-3 delivery systems has been evaluated in a wide range of food products (e.g., dressings, baked products or meat products) (Ghelichi et al., 2021). However, initial lipid oxidation is susceptible to occur during emulsification (e.g., air/oxygen inclusion and distribution) and subsequent spray-drying by using inlet air at high temperature (e.g., 160–200 °C) (Serfert et al., 2009). Therefore, in the last decades, significant progress has been made in the development of non-thermal encapsulation techniques such as electro-spraying to produce dry omega-3 delivery systems. By conventional

* Corresponding authors.

E-mail addresses: norelenarm@ugr.es (N.E. Rahmani-Manglano), pjgarcia@ugr.es (P.J. García-Moreno).

<https://doi.org/10.1016/j.foodchem.2023.136894>

Received 11 May 2023; Received in revised form 22 June 2023; Accepted 13 July 2023

Available online 17 July 2023

0308-8146/© 2023 The Authors. Published by Elsevier Ltd. This is an open access article under the CC BY-NC-ND license (<http://creativecommons.org/licenses/by-nc-nd/4.0/>).

electrospraying, the fish oil-loaded emulsion/dispersion is dried by means of the high-electrostatic field applied, which produces a spray of highly charged droplets allowing solvent evaporation at room temperature (Gómez-Mascaraque & López-Rubio, 2016). Furthermore, in the coaxial configuration, fish oil-loaded capsules can be produced without first emulsifying or dispersing the oil within the (bio)polymer-based encapsulating solution since two immiscible solutions can be simultaneously electrosprayed (Rahmani-Manglano et al., 2023). Thus, by electrospraying technology, initial lipid oxidation due to processing could be significantly reduced or even theoretically avoided, depending on the emitter configuration (e.g., monoaxial or coaxial configuration). Moreover, as a result of electrohydrodynamic atomization, smaller dry particles are produced compared to spray-drying, and the particle size distribution is also narrower (García-Moreno et al., 2021). This is desirable when it comes to food fortification since smaller capsules are easier to disperse in the food matrix and the structure of the original foodstuff is expected to be less modified. Nonetheless, it should be born in mind that an increased specific surface area of the electrosprayed encapsulates might result in a lower oxidative stability of the system due to a higher contact area with prooxidants species (e.g., oxygen).

In a recent study, we investigated the oxidative stability of fish oil-loaded capsules produced by spray-drying or electrospraying in the monoaxial and the coaxial configuration (Rahmani-Manglano et al., 2023). Interestingly, our results suggested that the physicochemical properties of the encapsulated systems (e.g., particle size or thickness of the encapsulating wall) played a major role on lipid oxidation. This might be attributed to its effect on oxygen permeability, which was not investigated.

Electron spin resonance (ESR) has been proven to be a useful technique to measure oxygen concentrations in food systems (ESR-based oximetry) (Zhou et al., 2011). This technique is based on the broadening of the ESR spectra of stable radicals (i.e., paramagnetic spin probes) in the presence of other paramagnetic molecule such as oxygen. The interaction between the spin probe and oxygen produces a spin exchange between these two compounds (e.g., Heisenberg spin exchange) resulting in the line broadening of the ESR spectra, which is proportional to the concentration of oxygen (M.L. Andersen, 2021). This technique has been previously used to evaluate the oxygen-barrier properties of oil-loaded encapsulated systems produced by different technologies (e.g., freeze-drying or electrospraying) (A.B. Andersen et al., 2000; Boerekamp et al., 2019; Svagan et al., 2016). Furthermore, the ESR technique has been also extensively used to monitor the early stages of lipid oxidation (ESR-spin trapping) of bulk, emulsified or encapsulated oils (M.L. Andersen, 2021). ESR-spin trapping relies in the formation of stable radicals (spin adducts) due to the reaction of free radicals and a diamagnetic molecular spin trap (usually nitrones or nitroso compounds), which allows the indirect measurement of the highly reactive intermediate lipid-derived radicals (e.g., alkyl radicals) (M.L. Andersen, 2021; Velasco et al., 2021).

Therefore, this study aimed at investigating the oxygen permeability fish oil-loaded capsules produced by spray-drying or electrospraying by using ESR-oximetry. Furthermore, the oxidative stability of the capsules was also studied by ESR-spin trapping during 25 days of storage at ambient temperature. To our knowledge, this is the first study comparing the oxidative stability and the oxygen permeability of fish oil-loaded capsules produced by spray-drying and electrospraying measured by ESR. The results obtained from this work advance our understanding on the relation of lipid oxidation in encapsulated systems and their physicochemical properties influencing oxygen diffusivity through the encapsulating wall.

2. Materials and methods

2.1. Materials

Fish oil (Omega Oil 1812 TG Gold) was purchased from BASF

Personal Care and Nutrition GmbH (Illertissen, Germany) and stored at $-80\text{ }^{\circ}\text{C}$ until use. MCT oil (WITARIX® MCT 60/40) was kindly donated by IOI OLEO GmbH (Hamburg, Deutschland) and stored at $-20\text{ }^{\circ}\text{C}$ until use. Glucose syrup (GS; DE38, C*Dry 1934) was purchased from Cargill Germany GmbH (Krefeld, Germany) and Pullulan was kindly donated by Hayashibara Co., Ltd. (Okayama, Japan). Tween 20 (T20) was obtained from Sigma-Aldrich (Darmstadt, Germany) and CITREM (GRINDSTED® CITREM LR 10 EXTRA MT) was provided by Danisco (Copenhagen, Denmark). Whey protein concentrate hydrolysate (WPCH) was produced by enzymatic hydrolysis (degree of hydrolysis, DH of 10%) with Alcalase 2.4L (Novozymes, Denmark) (Rahmani-Manglano et al., 2020). The hydrolysate was then freeze-dried and stored at $4\text{ }^{\circ}\text{C}$ until use. ESR spin probe (16-DOXYL-stearic acid, DSA) and spin trap (α -Phenyl-*N*-tert-butyl nitron, PBN) were purchased from Sigma Aldrich (Søborg, Denmark). Oxygen ($\geq 99.5\%$) and nitrogen ($\geq 99.999\%$) gases were supplied by Air Liquide (Taastrup, Denmark). The rest of the reagents used for analysis were of analytical grade.

2.2. Preparation of the ESR spin trap and spin probe

The ESR spin trap (PBN) and spin probe (DSA) were prepared and added to the lipid phase (fish oil and MCT oil, respectively), as described by Boerekamp et al. (2019). In brief, to investigate the oxidative stability of the encapsulated systems, PBN was added to the fish oil as an ethanolic solution (50 mg/mL) in order to have a final concentration of 30 mM of PBN in the lipid phase. For the oxygen permeability measurements, DSA was added to the MCT oil as a hexadecane solution (25 mg/mL) in order to have a final concentration of 10 μM of DSA in the lipid phase. MCT oil was used for the oxygen permeability measurements since it is a non-oxidizable oil which does not react with oxygen or with the spin probe. Thus, the broadening in the ESR signal of DSA would only be due to the change of oxygen concentrations inside the encapsulated oil droplets (Boerekamp et al., 2019).

2.3. Production of the spray-dried capsules

The oil-in-water emulsions were prepared by dispersing the lipid phase (MCT oil or fish oil, 5 wt%) in the aqueous phase containing the encapsulating agent (GS, 28 wt%) and the emulsifier (WPCH, 6 wt%). The protein/oil ratio was fixed at 0.4. First, a coarse emulsion was produced using an Ultraturrax T-25 homogenizer (IKA, Staufen, Germany) mixing at 15,000 rpm. The total mixing time was 2 min and the fish oil was added during the first minute. Then, the pre-emulsion was homogenized in a high-pressure homogenizer (PandaPLUS 2000; GEA Niro Soavi, Lübeck, Germany) at a pressure range of 450/75 bar and applying 3 passes. Right after production, the emulsions were spray-dried in a laboratory scale spray-drier (Büchi B-190; Büchi Labor-technik, Flawill, Switzerland) at 180/90 $^{\circ}\text{C}$ inlet/outlet temperature, respectively. The drying air flow was fixed to 25 Nm^3/h . The oil load of the resulting encapsulates was of $\sim 13\text{ wt}\%$. The capsules were stored in airtight flasks, at $-80\text{ }^{\circ}\text{C}$ in the dark until further analysis.

2.4. Production of the electrosprayed capsules

2.4.1. Production of monoaxially electrosprayed capsules

To produce the oil-in-water emulsions, a mixture of CITREM (1 wt %):oil (MCT oil or fish oil, 3.7 wt%) was dispersed in the aqueous phase as described in Section 2.3. The aqueous phase consisted of WPCH (4.3 wt%), P (3.0 wt%) and the encapsulating agent (GS, 15 wt%), which were previously dissolved in distilled water and stirred overnight (500 rpm) at ambient temperature. The resulting oil-in-water emulsions also had a protein/oil ratio of 0.4. Immediately after production, the emulsions were electrosprayed in the equipment described in our previous study (Rahmani-Manglano et al., 2023) consisting of a drying chamber equipped with a variable high-voltage power supply, a syringe pump, and a stainless-steel collector plate (SpinBox Electrospinning; Bioinicia,

Valencia, Spain). The flow rate was fixed to 0.2 mL/h and the voltage applied varied from 18.5 to 20 kV. The electrospaying process was carried out at ambient temperature and ambient relative humidity (19–23 °C, 22–50 % RH) in batches of 30 min. Between batches, the remaining emulsions were gently stirred (100 rpm) to minimize physical destabilization. The powder collected from the different batches was gently mixed to ensure that analyzed samples were homogeneous and representative of the obtained material. The final oil load of the capsules was ~13 wt%. The capsules were stored in airtight flasks, at –80 °C in the dark until further analysis.

2.4.2. Production of coaxially electrospayed capsules

For coaxial electrospaying, the biopolymer solution (flowing through the outer capillary) was produced by dissolving the encapsulating agent (GS, 15 wt%), P (4 wt%) and T20 (1 wt%) in distilled water and stirring overnight (500 rpm). Afterwards, the solution was passed through a high-pressure homogenizer (450/75 bar, 3 passes) prior to electrospaying. MCT oil or fish oil were infused as the core solutions (flowing through the inner capillary). The electrospaying process was carried out in the setup described in Section 2.4.1, equipped with coaxial emitter consisting of two concentric needles. Thus, two syringe pumps which worked simultaneously were used. The outer flow rate (F1) was fixed to 0.60 mL/h and the inner flow rate (F2) was adjusted to achieve a final oil load of the capsules of ~13 wt% (F2 = 0.021 mL/h). The voltage was varied from 16 to 18 kV. The process was conducted at ambient temperature and ambient relative humidity (19–23 °C, 22–50 % RH) in batches of 60 min. The powder collected from the different batches were gently mixed before sampling to ensure that analyzed samples were homogeneous and representative of the obtained material. The capsules were stored in airtight flasks, at –80 °C in the dark until further analysis.

2.5. Characterization of the capsules

2.5.1. Morphology and particle size distribution

The morphology of the capsules was investigated by scanning electron microscopy (SEM) using a FESEM microscope (LEO 1500 GEMINI, Zeiss, Germany). The samples were placed on carbon tape and carbon-coated as described in our previous work (Rahmani-Manglano et al., 2023). The SEM images were acquired in the range 500X – 15KX magnification with a 5-kV accelerating voltage. The particle size distributions and mean diameters were determined measuring 160 randomly-selected capsules using the ImageJ software (National Institute of Health).

2.6. ESR measurements

The ESR spectra of the encapsulated systems containing the spin trap (PBN) or the spin probe (DSA) were recorded using a MiniScope MS5000 (Bruker, Rheinstetten, Germany) at ambient temperature. The modulation amplitude used in all ESR measurements was kept constant in each determination at 0.2 mT.

2.6.1. Oxidative stability

To evaluate the oxidative stability of the capsules, the ESR tubes (5 mm OD) were filled with powder to obtain a sample height of ~3.5 cm in order to ensure that the resonant cavity of the equipment was covered with sample (Velasco et al., 2021). Thus, the volume of capsules was kept constant for the analyses. Three tubes were prepared per sample and subsequently stored at 25 °C in the dark for 25 days. The PBN-ESR spectra were recorded every day to monitor the changes in the peak-to-peak height of the central line of the spectra. For comparative purposes among capsules, the peak-to-peak amplitude measured for each sample was divided by the density in the ESR tubes of each capsule type (mg sample/cm tube). Thus, normalized values for peak-to-peak amplitude were obtained. The average value of the normalized peak-to-peak height of every sample was calculated.

2.6.2. Oxygen permeability

The oxygen permeability of the capsules was determined as described by Boerekamp et al. (2019). In brief, 200 mg of capsules were placed in quartz ERS tubes which were closed at one end with glass wool. Afterwards, the capsules were washed with heptane (10 mL) to remove the non-encapsulated surface oil fraction. For the measurements, first nitrogen (59.50 mL/min) was passed through the sample-containing tubes for 60 min to displace oxygen. Then, oxygen (50.49 mL/h) was passed through the tubes until the nitrogen atmosphere was completely replaced. By last, nitrogen (59.50 mL/min) was passed again through the tubes for 60 min. During the analysis, the narrowing (when nitrogen was passed through the tubes) and the broadening (when oxygen was passed through the tubes) of the ESR signal of DSA was quantified as the width of the central line of the spectra, ΔH_{pp} (Boerekamp et al., 2019; Svagan et al., 2016).

In addition, a calibration curve ($R^2 = 0.98$) was constructed to relate the line broadening of the DSA-ESR spectra (ΔH_{pp}) with the concentration of oxygen (Boerekamp et al., 2019). A piece of filter paper was soaked in the MCT oil containing the DSA probe (prepared as described in Section 2.2) and placed in the ESR quartz tube. First, a nitrogen atmosphere was created by passing nitrogen through the filter-containing tube for 15 min. Then, the filter paper was exposed to different oxygen/nitrogen gas compositions and the ΔH_{pp} was quantified to construct the calibration curve. Each point of the calibration curve was measured in triplicate.

2.7. Statistical analysis

Data were subjected to one-way analysis of variance (ANOVA) by using Statgraphics version 5.1 (Statistical Graphics Corp., Rockville, MD, USA). Tukey's HSD multiple range test was used at 95% confidence level ($p < 0.05$) to determine significant differences between mean values.

3. Results and discussion

3.1. Characterization of the capsules

3.1.1. Morphology and particle size distribution

Depending on the technology used (e.g., spray-drying or monoaxial/coaxial electrospaying), significant differences were observed on the morphology (Fig. 1) and particle size distribution (Fig. 2) of the encapsulated systems. Whilst spherical particles were obtained by spray-drying (Fig. 1A,B), fibrils interconnecting the capsules were observed for the electrospayed systems, irrespective of the emitter configuration (e.g., monoaxial or coaxial; Fig. 1C,D or Fig. 1E,F, respectively). This is ascribed to the presence of pullulan as thickening agent in the formulation of the electrospayed capsules (GS-mo and GS-HPH-co samples) which, due to its great spinnability in water-based solutions, leads to the formation of thin fibrils even at low concentrations (e.g., <5 wt% pullulan) (García-Moreno et al., 2018; Rahmani-Manglano et al., 2023). Nonetheless, as reported in our previous work, the electrospayed capsules had the appearance of flowing powder once the samples were detached from the collector (Rahmani-Manglano et al., 2023). Emulsion-based methods let to capsules with mostly smooth surfaces and the morphology of the particles was similar irrespective of the encapsulated oil (e.g., fish oil or MCT oil) (Fig. 1A-D). Conversely, in line with our previous observations (Rahmani-Manglano et al., 2023), coaxial electrospaying resulted in dented particles when fish oil was infused as the core solution (Fig. 1E). However, agglomerated capsules were observed when the core solution consisted of MCT oil (Fig. 1F). This could be explained due to the different polarities of the encapsulated oils (e.g., fish oil or MCT oil). MCT oil is more polar than fish oil (Chen et al., 2023) thus, in the absence of emulsifiers in the shell solution together with the lack of surface-active properties of the encapsulating agent (e.g., GS), a portion of the infused oil might have solubilized

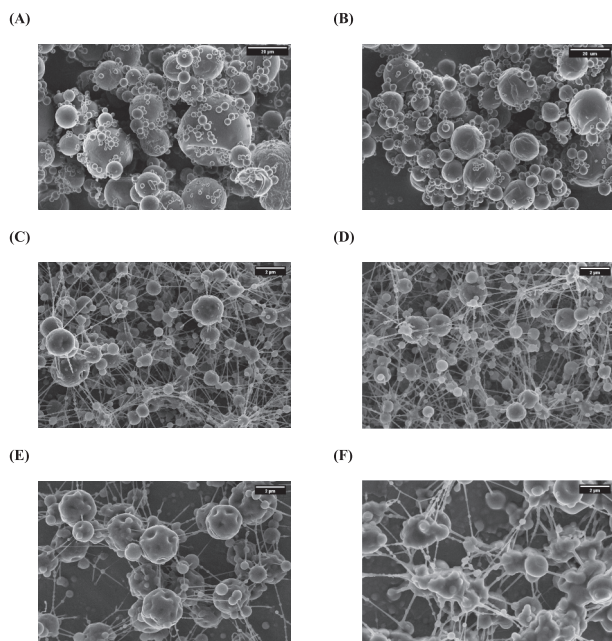


Fig. 1. SEM images of the oil-loaded capsules produced by: spray-drying (fish oil, **A**; MCT oil, **B**), monoaxial electrospinning (fish oil, **C**; MCT oil, **D**) and coaxial electrospinning (fish oil, **E**; MCT oil, **F**). The scale bar of the spray-dried capsules (**A**, **B**) corresponds to 20 μm . The scale bar of the electrospun capsules (monoaxial; **C**, **D** or coaxial; **E**, **F**) corresponds to 2 μm .

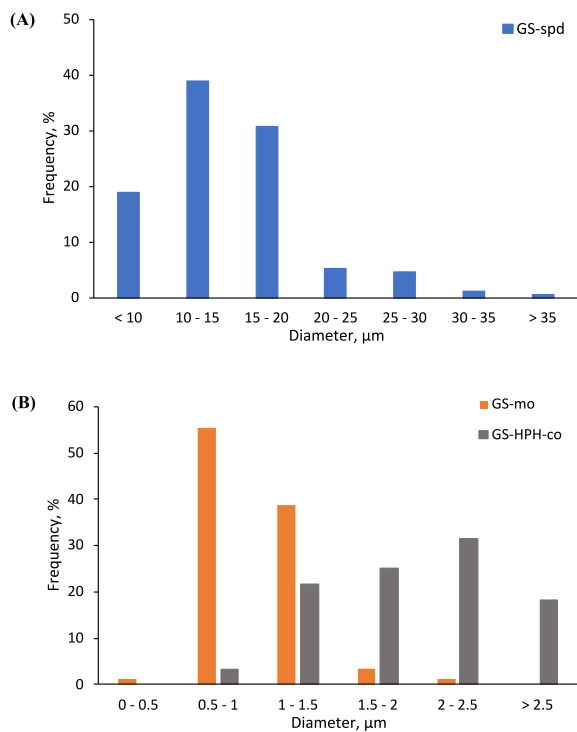


Fig. 2. Particle size distribution of the fish oil-loaded capsules produced by spray-drying (**A**) and electrospinning (monoaxial and coaxial) (**B**).

in the water-based encapsulating solution during processing giving rise to the agglomerated-like morphology of the resulting particles.

Fig. 2 shows the particle size distribution of the fish oil-loaded systems. Spray-drying resulted in significantly larger capsules and a wider particle size distribution ($p > 0.05$; **Fig. 2A**), compared to electrospinning (monoaxial or coaxial) (**Fig. 2B**). In turn, monoaxially electrospun capsules were smaller ($\sim 90\%$ of the capsules $< 1.5 \mu\text{m}$) than coaxially electrospun systems ($\sim 25\%$ of the capsules $< 1.5 \mu\text{m}$) due to the difference in the operating conditions (e.g., higher infusing flow rate for coaxial electrospinning) (Rahmani-Manglano et al., 2023). The particle size of oil-loaded encapsulated systems is an important factor influencing their oxidative stability since, for a fixed oil load, a reduced particle size implies an increased specific surface area (e.g., higher area of contact with prooxidant species) and thinner encapsulating walls (e.g., reduced prooxidants diffusion path to the core of the capsules) (Linke, Hinrichs, et al., 2020).

3.2. Oxidative stability

The PBN-ESR spectra of the fish oil-loaded capsules showed three

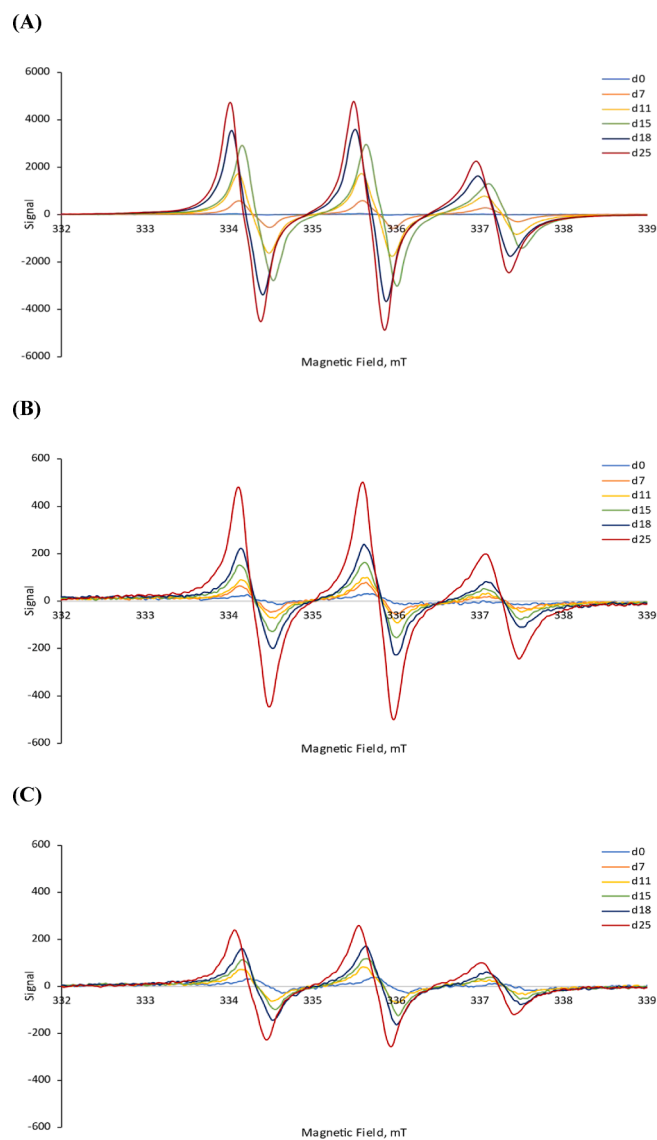


Fig. 3. Evolution of ESR spectra of the fish oil-loaded capsules containing the PBN spin trap during storage at 25 $^{\circ}\text{C}$. Capsules were produced by spray-drying (**A**), monoaxial electrospinning (**B**) and coaxial electrospinning (**C**).

broad lines (Fig. 3), in line with the PBN-ESR spectrum of neat fish oil (Fig. S1 of the Supplementary Material). These results are consistent with those reported by other authors for the ESR spectra of PBN-adducts formed in bulk, emulsified and encapsulated oils, where the typical coupling of nitroxyl radicals, but not the hydrogen splitting, was observed (Boerekamp et al., 2019; Velasco et al., 2005, 2021). As to the lipid-derived-radicals concentration is considered to be proportional to ESR signal intensity, the peak-to-peak amplitude of the central line of the PBN-ESR spectrum was used to monitor the lipid oxidation of the capsules (Boerekamp et al., 2019; Velasco et al., 2005). Fig. 3 and Fig. 4 show the evolution of the PBN-ESR spectra and the evolution of peak-to-peak amplitude of the encapsulated systems over storage, respectively. Significantly different trends were observed in both figures depending of the technology used to produce the capsules (e.g., spray-drying, monoaxial electro-spraying or coaxial electro-spraying).

At the beginning of the storage time, low but detectable levels of radicals were found in all the samples (Fig. 3), contrary to the neat fish oil (Fig. S1 of the Supplementary Material). These results suggest that lipid oxidation already occurred during the encapsulation process, irrespective of the technology used (Velasco et al., 2021). However, although the PBN-ESR signal detected for the fish oil-loaded capsules after processing appeared similar among the samples (Fig. 3), the normalized signal of the spray-dried capsules was smaller after correcting for the different densities of sample in the ESR tubes (Fig. 4). During storage, the ESR signal intensity of the spray-dried capsules showed a lag-phase of 4 days, followed by a sharp increase up to day 21. Afterwards, a slower increase in the peak-to-peak amplitude was noted and the ESR signal intensity decreased by the end of the storage time (Fig. 4). Nonetheless, the opposite trend was found for the electro-sprayed systems (e.g., monoaxial, GS-mo and coaxial, GS-HPH-co) (Fig. 4) for which a small and rather constant peak-to-peak amplitude was observed during storage. Although it is widely accepted that high levels of radicals detected by ESR spin trapping indicate high levels of oxidation, the interpretation of our results might not be as straightforward. The detection of lipid radicals depends on several factors such as the formation rate and stability of the radical to be trapped, the rate of trapping and the stability of the spin adducts formed (Velasco et al., 2021). In addition, it has been reported that ESR spin trapping experiments should be limited to the early stages of lipid oxidation (Merckx et al., 2021; Velasco et al., 2005). Spin adducts are radicals themselves, thus they can react with other lipid-derived-radicals in conditions of advanced lipid oxidation (where their concentration is rather high) giving rise to ESR-silent compounds (e.g., diamagnetic species) (M.L. Andersen, 2021; Velasco et al., 2005). Therefore, low levels of lipid radicals might be measured in oxidized samples (M.L. Andersen, 2021). This is in agreement with previous studies that investigated the development of PBN-spin adducts at early and advanced stages of lipid oxidation in bulk oils or in oil-encapsulated systems (Falch et al., 2005;

Velasco et al., 2021). In case of bulk oils (Falch et al., 2005), the lowest concentration of radicals observed corresponded to the sample that oxidized more rapidly during storage, as confirmed by the PV and TBARS measurements. Furthermore, radicals decay occurred significantly earlier compared to the more oxidatively stable oil and after that time, a low and rather constant concentration of PBN-adducts was observed until the end of the storage time (Falch et al., 2005). In a recent study, the same trend observed for bulk oils was reported for oil-loaded encapsulated systems (Velasco et al., 2021). The lowest concentration of radicals was found for the samples that were proven to oxidize more rapidly, and their concentration, after the decay of radicals occurred, did not significantly vary during the storage time. Moreover, for the less oxidatively stable encapsulated system, an initial formation of radicals followed by a decay was not noted. It was attributed to a rapid lipid oxidation during the early stages of incubation since the rate of radicals' depletion was higher than the rate of radicals' formation (Velasco et al., 2021). Taken altogether, our results suggest that the electro-sprayed systems (GS-mo and GS-HPH-co samples) produced in the current study oxidized faster than those produced by spray-drying (GS-spd). Indeed, these results are in agreement with those reported in our previous study (Rahmani-Manglano et al., 2023), where a significantly higher oxidative stability was observed for the spray-dried capsules compared to the electro-sprayed systems (monoaxial and coaxial), as confirmed by FT-IR measurements and the development of secondary volatile oxidation products during storage. These findings were explained due to potential differences in oxygen permeability of the encapsulated systems, which was further investigated in this study.

3.3. Oxygen permeability

Lipid autoxidation occurs as a chain reaction between lipid radicals (e.g., alkyl radicals) and oxygen (Johnson & Decker, 2015). Thus, to promote lipid oxidation of encapsulated systems, it is assumed that the environmental oxygen has to get in contact with the encapsulated oil droplets (Linke, Hinrichs, et al., 2020). Indeed, in the literature, oxygen diffusivity through the encapsulating wall has been extensively pointed out to be the key factor influencing lipid oxidation of encapsulated oils (Boerekamp et al., 2019; Drusch et al., 2009; Linke et al., 2021, 2022; Linke, Linke, et al., 2020; Linke, Weiss, et al., 2020; Velasco et al., 2006). Nonetheless, to our knowledge, there are not studies comparing the oxygen permeability of spray-dried and electro-sprayed encapsulated systems neither its influence on oxidative stability.

To evaluate the oxygen-barrier properties of the encapsulating matrices, the capsules were first washed with heptane to suppress the DSA-ESR signal arising from the easily oxygen-accessible non-encapsulated oil fraction. The DSA-ESR spectra of the non-oxidizing MCT oil-loaded capsules after washing produced by spray-drying (GS-spd) and monoaxial electro-spraying (GS-mo) are shown in Fig. 5, where three lines can be distinguished (e.g., high field line, central line and low field line). However, a flat ESR spectrum was obtained for the capsules produced by coaxial electro-spraying after washing (Fig. S2 of the Supplementary Material). The latter indicates that washing with heptane the coaxially electro-sprayed capsules not only removed the non-encapsulated oil fraction, but most of the MCT oil containing the DSA probe. By optimal coaxial electro-spraying, the oil is theoretically located at the core of the capsule as a single droplet surrounded by the encapsulating wall. Therefore, if the matrix is not completely solid, the encapsulated oil fraction can be easily reached, and thereby extracted, by the washing solvent that diffuses through capillary or cracks present on the surface of the capsules (Drusch & Berg, 2008). As a result, the oxygen permeability of the coaxially electro-sprayed capsules (GS-HPH-co sample) could not be evaluated in the current study by ESR technology. However, our results could be regarded as an indication of the higher oxygen permeability of the coaxially electro-sprayed capsules compared to those produced by the emulsion-based methods (e.g., spray-drying and monoaxial electro-spraying), for which the extraction

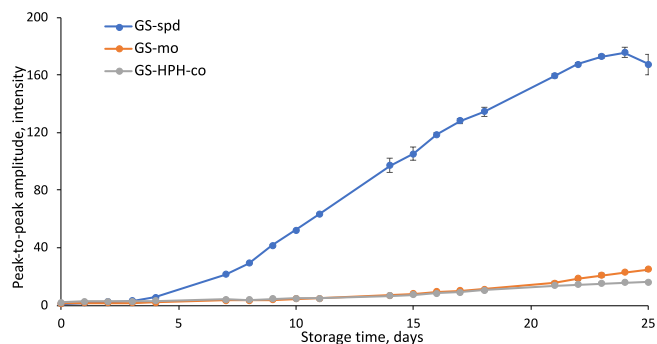


Fig. 4. Peak-to-peak amplitude of the central line of the PBN-ESR spectra of the fish oil-loaded capsules containing the PBN spin trap as a function of storage time at 25 °C. Capsules were produced by spray-drying (GS-spd), monoaxial electro-spraying (GS-mo) and coaxial electro-spraying (GS-HPH-co).

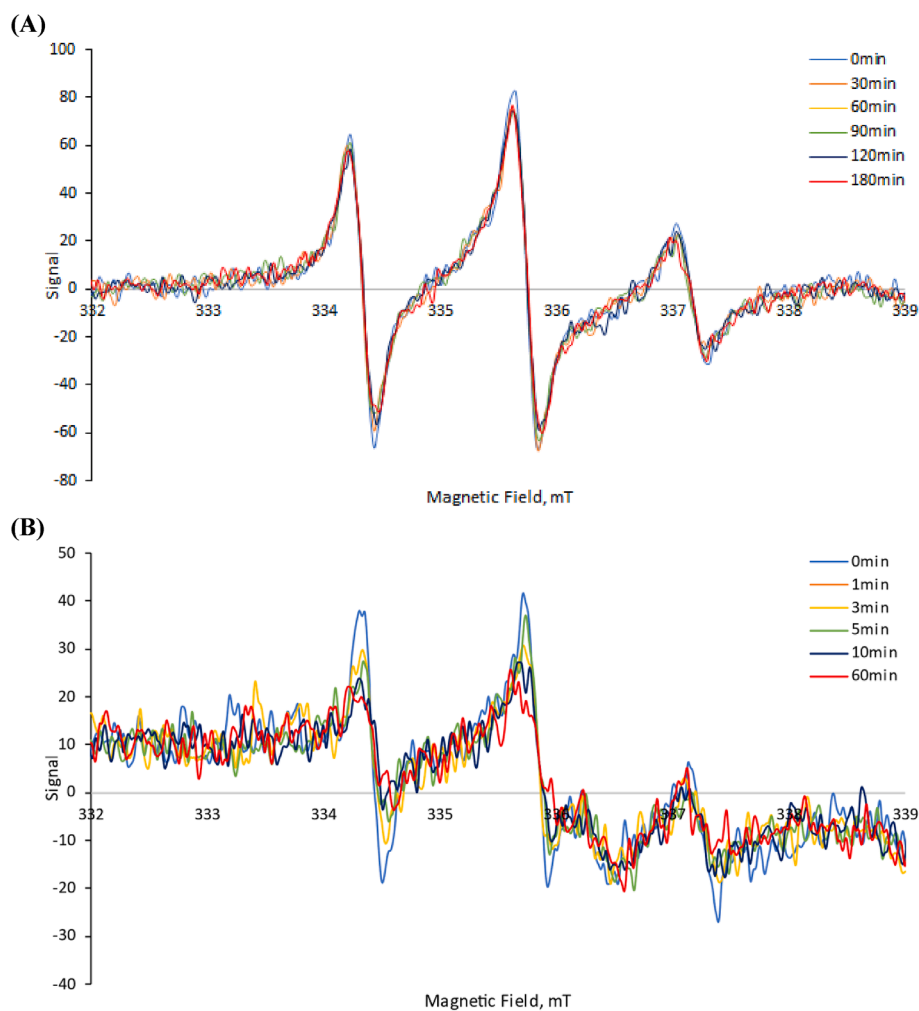


Fig. 5. Evolution of the DSA-ESR spectrum of the MCT oil-loaded capsules containing the DSA probe produced by spray-drying (A) and monoaxial electrospaying (B) as the pure nitrogen atmosphere was changed to a pure oxygen atmosphere.

of entrapped oil did not occur during washing with heptane.

It should be noted that the DSA probe in pure MCT oil also showed a three-line spectrum (Fig. S3A of the Supplementary Material) which were similar to the DSA-ESR spectra of the encapsulated systems (GS-spd and GS-mo samples; Fig. 5). This suggests that the DSA lipophilic probe was mainly located in the oil phase of the capsules, and therefore the broadening of the central line width (ΔH_{pp}) of the DSA-ESR spectrum of the encapsulated systems occurred as a consequence of the interaction of the DSA probe and the oxygen dissolved in the oil (A.B. Andersen et al., 2000; Boerekamp et al., 2019; Svagan et al., 2016).

As shown in Fig. 5, changing the atmosphere from pure nitrogen to pure oxygen resulted in the broadening of the central line (ΔH_{pp}), together with the decrease of the signal intensity with exposure time (Boerekamp et al., 2019). The changes in the DSA-ESR spectrum of the capsules produced by monoaxial electrospaying (GS-mo sample) were more extensive compared to that of the spray-dried capsules (GS-spd) (Fig. 5). Fig. 6 shows the narrowing and the broadening of the central line width (ΔH_{pp}) with time upon exposure to nitrogen or oxygen atmospheres, respectively. At time zero, the atmosphere was changed from environmental air to nitrogen (i.e., the first data recorded corresponded to environmental air) and the samples were equilibrated for 1 h under nitrogen exposure. After this time, the atmosphere was changed from nitrogen to oxygen until the steady-state was reached, indicating that the oxygen dissolved in the encapsulated oil was in equilibrium with the surrounding atmosphere of pure oxygen. Then, the capsules were again exposed to pure nitrogen for 1 h (Fig. 6). Both encapsulated

systems presented a relatively high ΔH_{pp} initial value ($p > 0.05$; Fig. 6), suggesting that a high oxygen content was already present in the encapsulated oil (A.B. Andersen et al., 2000) which can be mainly attributed to air inclusion occurring during emulsification, drying and storage. However, although the initial ΔH_{pp} values were close among the samples, their evolution with gas exposure time was significantly different depending on the technology used to produce the capsules. As expected, upon nitrogen exposure, the central line of the spectra narrowed for both systems but the limiting ΔH_{pp} values reached were different (Fig. 6). According to the standard curve (Fig. S3B of the Supplementary Material), spray-dried capsules reached an asymptotic ΔH_{pp} value of 0.24 ± 0.01 mT corresponding to a situation where the encapsulated oil is in equilibrium with an atmosphere containing ~53% nitrogen. On the contrary, our results show that the oil contained in GS-mo sample was in equilibrium with the surrounding nitrogen atmosphere (100% nitrogen) after 1 h ($\Delta H_{pp} = 0.19 \pm 0.01$ mT). This suggests higher permeability to nitrogen of the electrospayed capsules compared to spray-dried capsules. Accordingly, the central line width (ΔH_{pp}) of both encapsulated systems increased with time when these were exposed to pure oxygen, but the broadening rate was again significantly different among the samples (Fig. 6). For the spray-dried capsules, a rapid increase of the central line width (ΔH_{pp}) was observed during the early stages of oxygen exposure (~20 min) followed by sustained increase until an asymptotic value was reached after ~2 h ($\Delta H_{pp} = 0.29 \pm 0.01$ mT). Due to the heterogeneous nature of emulsion-based encapsulating systems, in which the oil droplets are randomly

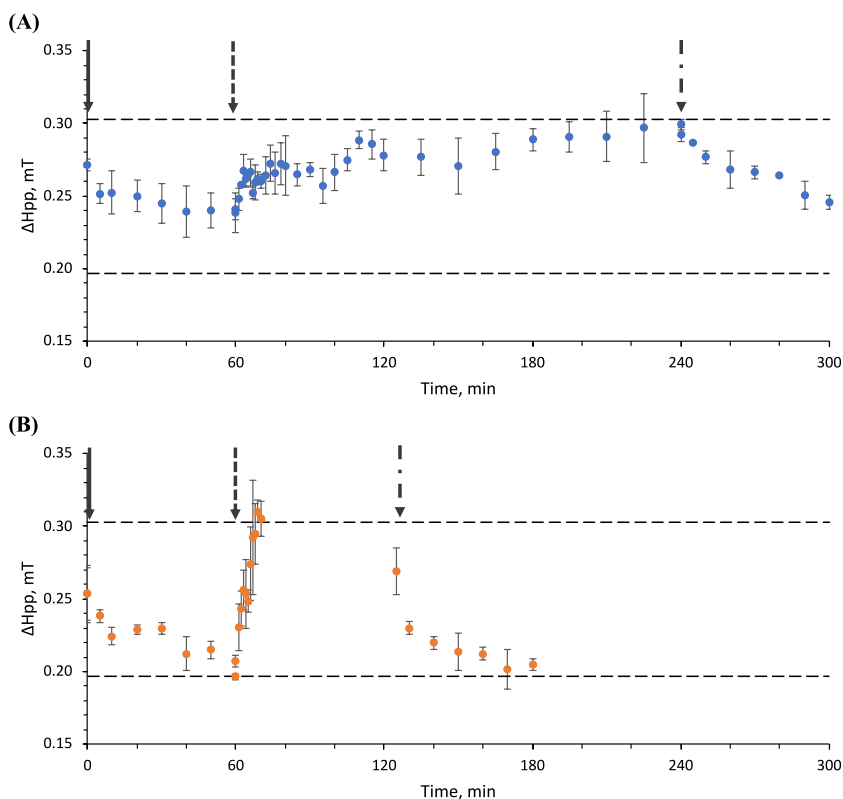


Fig. 6. Broadening of the central line width (ΔH_{pp}) of the DSA-ESR spectrum of the MCT oil-loaded capsules containing the DSA probe produced by spray-drying (GS-spd) (A) or monoaxial electrospinning (GS-mo) (B) with time. The dashed lines represent the maximum (upper line) and minimum (lower line) line width (ΔH_{pp}) of the DSA-ESR spectrum in pure MCT oil, according to the standard curve. The solid arrow marks when the atmosphere was changed from environmental air to pure nitrogen. The dashed arrow marks when the atmosphere was changed from pure nitrogen to pure oxygen. The dotted arrow marks when the atmosphere was changed from pure oxygen to pure nitrogen.

distributed within the glassy encapsulating wall, a gradient in oxygen concentration inside the matrix is expected depending on the properties of the encapsulating wall and the distribution and size of the oil droplets (A.B. Andersen et al., 2000; Linke, Hinrichs, et al., 2020). Thus, the sharp increase of ΔH_{pp} observed upon early oxygen exposure can be ascribed to the contribution of the oil droplets located near the surface of the spray-dried capsules that came fast into contact with the penetrating oxygen due to the difference in partial pressure outside and inside the capsules. Afterwards, the rate of the central line broadening decay as the oxygen concentration increased inside the capsules until the equilibrium with the surrounding oxygen atmosphere was reached (e.g., the capsules were saturated with oxygen and the ΔH_{pp} remained unvaried) (Kak et al., 2019; Tikekar et al., 2011). Conversely, the ΔH_{pp} of the monoaxially electrospun capsules (GS-mo sample) increased exponentially and the equilibrium with the pure oxygen atmosphere was reached after 10 min ($\Delta H_{pp} = 0.30 \pm 0.01$ mT). Oxygen diffusivity in encapsulated systems depends on the size of the capsules and the thickness and nature of the encapsulating wall. Smaller capsules result in an increased surface-to-volume ratio, implying a higher particle-air interface and therefore a higher surface area available for the diffusion process (Linke, Hinrichs, et al., 2020; Rahmani-Manglano et al., 2023). Furthermore, the oxygen diffusion path to the core of the capsules is shorter for smaller capsules when the oil load is fixed (Linke, Hinrichs, et al., 2020). This is consistent with our findings where the significantly smaller capsules produced by monoaxial electrospinning ($p \leq 0.05$; Fig. 2) were significantly more permeable to oxygen than those produced by spray-drying (Fig. 6).

After changing the surrounding atmosphere from pure oxygen to pure nitrogen, the ΔH_{pp} decreased exponentially for both systems similarly as it was first observed when the atmosphere was changed from environmental air to pure nitrogen (Fig. 6). Indeed, the limiting ΔH_{pp} values reached after 1 h of nitrogen exposure at the end of the test agree with those obtained at the beginning for both systems (GS-spd and GS-mo samples; Fig. 6). Thus, whilst the capsules produced by monoaxial electrospinning were saturated with nitrogen at the end of the test (GS-

mo; Fig. 6B), a relatively high concentration of oxygen was still present in the capsules produced by spray-drying (GS-spd; Fig. 6A). The latter suggests that not only the properties of the spray-dried capsules prevented oxygen from permeating into the oil phase, but it also prevented oxygen from permeating out. Furthermore, the ΔH_{pp} narrowing rate of the capsules produced by spray-drying (Fig. 6), further confirming the higher gas permeability of GS-mo sample. Finally, it is also noteworthy that the ΔH_{pp} broadening rate of the spray-dried capsules was slower than the ΔH_{pp} narrowing rate when the sample was exposed to oxygen, and subsequently to nitrogen (Fig. 6A). This is once again ascribed to the heterogeneity of the encapsulated system since the random distribution of the oil droplets determine the interaction of the probe with the gases and, therefore, the ESR spectra (A.B. Andersen et al., 2000). Under non-steady state conditions, the recorded spectrum represents the sum of the individual ESR-spectra of the system that will vary the ΔH_{pp} , depending on the gas type (e.g., nitrogen and oxygen) and concentration (A.B. Andersen et al., 2000; Svagan et al., 2016). Furthermore, the recorded ESR spectra of heterogeneous systems are dominated by the narrow-line contributions of the DSA probe located in the oil droplets with low oxygen contents (A.B. Andersen et al., 2000; Svagan et al., 2016). Therefore, the faster ΔH_{pp} narrowing observed for the spray-dried capsules upon nitrogen exposure can be explained by the fast contact of the oil droplets located near the surface of the capsules with the penetrating nitrogen, which significantly influence the ΔH_{pp} of the recorded spectra (Boerekamp et al., 2019). However, for the capsules produced by monoaxial electrospinning, a fast and similar ΔH_{pp} broadening and narrowing rate were observed (Fig. 6B) as a consequence of the higher gas permeability of the matrix.

Although it is accepted that oxygen that is already present in the encapsulating matrix can contribute to lipid oxidation, the oxygen permeability through the encapsulating wall has been reported to be more important in determining the overall rate and extent of lipid oxidation (Linke et al., 2022; Linke, Linke, et al., 2020; Reineccius & Yan, 2016). Thus, encapsulating systems with low oxygen permeability

are expected to be more efficient in preventing lipid oxidation of the encapsulated oil. The latter is in agreement with our findings since the spray-dried capsules were proven to be significantly less permeable to oxygen which, in turn, correlates with the higher oxidative stability reported for this system measured by ESR in this work, as well as previously reported based on the measurement of secondary volatile oxidation products (Rahmani-Manglano et al., 2023).

4. Conclusions

The oxidative stability and the oxygen permeability of oil-loaded capsules produced by spray-drying or electro spraying (monoaxial or coaxial configuration) was investigated by means of ESR spectroscopy. The ESR-spin trapping results showed that spray-dried capsules oxidized slower during storage than those produced by electro spraying, irrespective of the emitter configuration. Moreover, ESR-oximetry results indicated that spray-dried capsules were more efficient in delaying gas permeability through the encapsulating matrix when compared to monoaxially electro sprayed capsules. This has been attributed to the larger particle size of the spray-dried capsules which results in a smaller surface-to-volume ratio and in thicker encapsulating walls (for the same oil load), both affecting the diffusion process. Overall, our results confirm the key role of oxygen permeability on the oxidative stability of fish oil-loaded capsules. This fact should be borne in mind for the development of oxidatively stable electro sprayed capsules loaded with oils rich in omega-3 PUFAs.

CRedit authorship contribution statement

Nor E. Rahmani-Manglano: Conceptualization, Methodology, Formal analysis, Writing – original draft. **Mogens L. Andersen:** Conceptualization, Methodology, Supervision, Writing – review & editing. **Emilia M. Guadix:** Conceptualization, Methodology, Supervision, Writing – review & editing, Funding acquisition. **Pedro J. García-Moreno:** Conceptualization, Methodology, Supervision, Writing – review & editing.

Declaration of Competing Interest

The authors declare that they have no known competing financial interests or personal relationships that could have appeared to influence the work reported in this paper.

Data availability

Data will be made available on request.

Acknowledgements

This work was supported by the I+D+i project CTQ2017-87076-R funded by MCIN/AEI/10.13039/501100011033/. N. E. Rahmani-Manglano acknowledges a FPI grant PRE2018-084861 funded by MCIN/AEI/10.13039/501100011033. The authors are grateful to Cristina Coronas for her help in producing the capsules and to Henriette Ribbjerg Erichsen for helping with the ESR experiments. Funding for open access charge: Universidad de Granada / CBUA.

Appendix A. Supplementary data

Supplementary data to this article can be found online at <https://doi.org/10.1016/j.foodchem.2023.136894>.

References

Andersen, A. B., Risbo, J., Andersen, M. L., & Skibsted, L. H. (2000). Oxygen permeation through an oil-encapsulating glassy food matrix studied by ESR line broadening

using a nitroxyl spin probe. *Food Chemistry*, 70(4), 499–508. www.elsevier.com/locate/foodchem.

- Andersen, M. L. (2021). Lipid oxidation studied by electron paramagnetic resonance (EPR). *Omega-3 delivery systems*. Elsevier Inc.. <https://doi.org/10.1016/b978-0-12-821391-9.00004-1>.
- Boerekamp, D. M. W., Andersen, M. L., Jacobsen, C., Chronakis, I. S., & García-Moreno, P. J. (2019). Oxygen permeability and oxidative stability of fish oil-loaded electro sprayed capsules measured by Electron Spin Resonance: Effect of dextran and glucose syrup as main encapsulating materials. *Food Chemistry*, 287, 287–294. <https://doi.org/10.1016/j.foodchem.2019.02.096>
- Chen, Y., Cheng, H., & Liang, L. (2023). Effect of oil type on spatial partition of resveratrol in the aqueous phase, the protein interface and the oil phase of O/W emulsions stabilized by whey protein and caseinate. *Antioxidants*, 12(3), 589. <https://doi.org/10.3390/antiox12030589>
- Drusch, S., & Berg, S. (2008). Extractable oil in microcapsules prepared by spray-drying: Localisation, determination and impact on oxidative stability. *Food Chemistry*, 109(1), 17–24. <https://doi.org/10.1016/j.foodchem.2007.12.016>
- Drusch, S., Rätzke, K., Shaikh, M. Q., Serfert, Y., Steckel, H., Scampicchio, M., ... Mannino, S. (2009). Differences in free volume elements of the carrier matrix affect the stability of microencapsulated lipophilic food ingredients. *Food Biophysics*, 4(1), 42–48. <https://doi.org/10.1007/s11483-008-9100-9>
- Falch, E., Velasco, J., Aursand, M., & Andersen, M. L. (2005). Detection of radical development by ESR spectroscopy techniques for assessment of oxidative susceptibility of fish oils. *European Food Research and Technology*, 221(5), 667–674. <https://doi.org/10.1007/s00217-005-0009-y>
- García-Moreno, P. J., Pelayo, A., Yu, S., Busolo, M., Lagaron, J. M., Chronakis, I. S., & Jacobsen, C. (2018). Physicochemical characterization and oxidative stability of fish oil-loaded electro sprayed capsules: Combined use of whey protein and carbohydrates as wall materials. *Journal of Food Engineering*, 231, 42–53. <https://doi.org/10.1016/j.jfoodeng.2018.03.005>
- García-Moreno, P. J., Rahmani-Manglano, N. E., Chronakis, I. S., Guadix, E. M., Yesiltas, B., Sørensen, A.-D.-M., & Jacobsen, C. (2021). Omega-3 nano-microencapsulates produced by electrohydrodynamic processing. In P. J. García-Moreno, C. Jacobsen, A.-D.-M. Sørensen, & B. Yesiltas (Eds.), *Omega-3 delivery systems. Production, physical characterization and oxidative stability* (pp. 345–370). Academic Press. <https://doi.org/10.1016/b978-0-12-821391-9.00017-x>.
- Ghelichi, S., Hajfathalian, M., García-Moreno, P. J., Yesiltas, B., Moltke-Sørensen, A.-D., & Jacobsen, C. (2021). Food enrichment with omega-3 polyunsaturated fatty acids. In P. J. García-Moreno, C. Jacobsen, A. D. M. Sørensen, & B. Yesiltas (Eds.), *Omega-3 Delivery Systems* (pp. 395–425). Academic Press. <https://doi.org/10.1016/b978-0-12-821391-9.00020-x>.
- Gómez-Mascaraque, L. G., & López-Rubio, A. (2016). Protein-based emulsion electro sprayed micro- and submicroparticles for the encapsulation and stabilization of thermosensitive hydrophobic bioactives. *Journal of Colloid and Interface Science*, 465, 259–270. <https://doi.org/10.1016/j.jcis.2015.11.061>
- Johnson, D. R., & Decker, E. A. (2015). The role of oxygen in lipid oxidation reactions: A review. *Annual Review of Food Science and Technology*, 6, 171–190. <https://doi.org/10.1146/annurev-food-022814-015532>
- Kak, A., Bajaj, P. R., Bhunia, K., Nitin, N., & Sablani, S. S. (2019). A fluorescence-based method for estimation of oxygen barrier properties of microspheres. *Journal of Food Science*, 84(3), 532–539. <https://doi.org/10.1111/1750-3841.14453>
- Linke, A., Hinrichs, J., & Kohlus, R. (2020). Impact of the powder particle size on the oxidative stability of microencapsulated oil. *Powder Technology*, 364, 115–122. <https://doi.org/10.1016/j.powtec.2020.01.077>
- Linke, A., Linke, T., & Kohlus, R. (2020). Contribution of the internal and external oxygen to the oxidation of microencapsulated fish oil. *European Journal of Lipid Science and Technology*, 1900381, 1900381. <https://doi.org/10.1002/ejlt.201900381>
- Linke, A., Teichmann, H., & Kohlus, R. (2022). Simulation of the oxidation of microencapsulated oil based on oxygen distribution – Impact of powder and matrix properties. *Powder Technology*, 401. <https://doi.org/10.1016/j.powtec.2022.117289>
- Linke, A., Weiss, J., & Kohlus, R. (2020). Oxidation rate of the non-encapsulated- and encapsulated oil and their contribution to the overall oxidation of microencapsulated fish oil particles. *Food Research International*, 127. <https://doi.org/10.1016/j.foodres.2019.108705>
- Linke, A., Weiss, J., & Kohlus, R. (2021). Impact of the oil load on the oxidation of microencapsulated oil powders. *Food Chemistry*, 341(September 2020). <https://doi.org/10.1016/j.foodchem.2020.128153>, 128153.
- Merkx, D. W. H., Plankensteiner, L., Yu, Y., Wierenga, P. A., Hennebel, M., & Van Duynhoven, J. P. M. (2021). Evaluation of PBN spin-trapped radicals as early markers of lipid oxidation in mayonnaise. *Food Chemistry*, 334. <https://doi.org/10.1016/j.foodchem.2020.127578>
- Orlien, V., Andersen, A. B., Sinkko, T., & Skibsted, L. H. (2000). Hydroperoxide formation in rapeseed oil encapsulated in a glassy food model as influenced by hydrophilic and lipophilic radicals. *Food Chemistry*, 68, 191–199. [https://doi.org/10.1016/S0308-8146\(99\)00177-6](https://doi.org/10.1016/S0308-8146(99)00177-6)
- Patel, A., Desai, S. S., Mane, V. K., Enman, J., Rova, U., Christakopoulos, P., & Matsakas, L. (2022). Futuristic food fortification with a balanced ratio of dietary ω-3/ω-6 omega fatty acids for the prevention of lifestyle diseases. In *Trends in food science and technology* (pp. 140–153). Elsevier Ltd.. <https://doi.org/10.1016/j.tifs.2022.01.006>
- Rahmani-Manglano, N. E., González-Sánchez, I., García-Moreno, P. J., Espejo-Carpio, F. J., Jacobsen, C., & Guadix, E. M. (2020). Development of fish oil-loaded microcapsules containing whey protein hydrolysate as film-forming material for fortification of low-fat mayonnaise. *Foods*, 9(5).

- Rahmani-Manglano, N. E., Guadix, E. M., Jacobsen, C., & García-Moreno, P. J. (2023). Comparative study on the oxidative stability of encapsulated fish oil by monoaxial or coaxial electrospraying and spray-drying. *Antioxidants*, *12*(2). <https://doi.org/10.3390/antiox12020266>
- Reineccius, G. A., & Yan, C. (2016). Factors controlling the deterioration of spray dried flavourings and unsaturated lipids. In *Flavour and Fragrance Journal* (pp. 5–21). John Wiley and Sons Ltd. Vol. 31, Issue 1 <https://doi.org/10.1002/ffj.3270>.
- Serfert, Y., Drusch, S., & Schwarz, K. (2009). Chemical stabilisation of oils rich in long-chain polyunsaturated fatty acids during homogenisation, microencapsulation and storage. *Food Chemistry*, *113*(4), 1106–1112. <https://doi.org/10.1016/j.foodchem.2008.08.079>
- Singh, H., Kumar, Y., & Meghwal, M. (2022). Encapsulated oil powder: Processing, properties, and applications. In *Journal of Food Process Engineering*, *45*. John Wiley and Sons Inc.. <https://doi.org/10.1111/jfpe.14047>.
- Svagan, A. J., Bender Koch, C., Hedenqvist, M. S., Nilsson, F., Glasser, G., Balushev, S., & Andersen, M. L. (2016). Liquid-core nanocellulose-shell capsules with tunable oxygen permeability. *Carbohydrate Polymers*, *136*, 292–299. <https://doi.org/10.1016/j.carbpol.2015.09.040>
- Tikekar, R. V., Johnson, A., & Nitin, N. (2011). Real-time measurement of oxygen transport across an oil-water emulsion interface. *Journal of Food Engineering*, *103*(1), 14–20. <https://doi.org/10.1016/j.jfoodeng.2010.08.030>
- Velasco, J., Andersen, M. L., & Skibsted, L. H. (2005). Electron spin resonance spin trapping for analysis of lipid oxidation in oils: Inhibiting effect of the spin trap α -phenyl-N-tert-butyl nitron on lipid oxidation. *Journal of Agricultural and Food Chemistry*, *53*(5), 1328–1336. <https://doi.org/10.1021/jf049051w>
- Velasco, J., Andersen, M. L., & Skibsted, L. H. (2021). ESR spin trapping for in situ detection of radicals involved in the early stages of lipid oxidation of dried microencapsulated oils. *Food Chemistry*, *341*(June 2020). <https://doi.org/10.1016/j.foodchem.2020.128227>, 128227.
- Velasco, J., Dobarganes, C., & Márquez-Ruiz, G. (2003). Variables affecting lipid oxidation in dried microencapsulated oils. *Grasas y Aceites*, *54*(3), 304–314.
- Velasco, J., Marmesat, S., Dobarganes, C., & Márquez-Ruiz, G. (2006). Heterogeneous aspects of lipid oxidation in dried microencapsulated oils. *Journal of Agricultural and Food Chemistry*, *54*(5), 1722–1729. <https://doi.org/10.1021/jf052313p>
- Zhou, Y. T., Yin, J. J., & Lo, Y. M. (2011). Application of ESR spin label oximetry in food science. In *Magnetic Resonance in Chemistry* (Vol. 49, Issue SUPPL. 1). <https://doi.org/10.1002/mrc.2822>